JOC Article

Extended Hypervalent 5c−6e Interactions: Linear Alignment of Five C−Se---O---Se−C Atoms in Anthraquinone and 9-Methoxyanthracene Bearing Arylselanyl Groups at the 1,8-Positions

Warô Nakanishi,* Satoko Hayashi, and Norio Itoh

Department of Chemistry and Material Science, Faculty of Systems Engineering, Wakayama University, 930 Sakaedani, Wakayama 640-8510, Japan

nakanisi@sys.wakayama-u.ac.jp

Received September 24, 2003

The structures of 1,8-bis(phenylselanyl)anthraquinone (**1a**), 1,8-bis(phenylselanyl)-9-methoxyanthracene (**2a**), and 1,8-bis(phenylselanyl)anthracene (**3a**) are determined by X-ray crystallographic analysis, together with the derivatives. The Se−C_i (Ph) bonds in **1a** are placed on the anthraquinone plane (both type **B**) and the phenyl planes are perpendicular to the anthraquinone plane. The structure around the Se atoms in **2a** is very close to that of **1a**: the conformations of the PhSe groups are both type **B**. Consequently, the five C_i−Se- - -O- - -Se−C_i atoms in **1a** and **2a** align linearly. The nonbonded Se- - -O distances in **1a** and **2a** are 2.673−2.688 and 2.731−2.744 Å, respectively, which are about 0.7 Å shorter than the sum of van der Waals radii of the atoms. The extended hypervalent σ^*(C_i−Se)- - -n_p(O)- - -σ^*(Se−C_i) 5c−6e interactions are strongly suggested for the origin of the linear alignment of the five atoms in **1a** and **2a**. The 5c−6e must be constructed by the connection of the two hypervalent n_p(O)- - -σ^*(Se−C_i) 3c−4e interactions through the central n_p(O). The five C_i−Se- - -H- - -Se−C_i atoms never align linearly in **3a**. To reveal the nature of 5c−6e in **1a** and **2a**, QC calculations are performed on $H_aH_b{}^A$Se- - -O(=CH_2)- - -^{B}Se$H_{a'}H_{b'}$ (model **a**) and $H_aH_b{}^A$Se- - -OH_2- - -^{B}Se$H_{a'}H_{b'}$ (model **b**) with the B3LYP/6-311++G(3df,2pd) method, where the nonbonded Se- - -O distances are fixed at 2.658 Å. Four conformers, **a** (**AA**-cis), **a** (**AA**-trans), **a** (**AB**), and **a** (**BB**), are optimized to be stable for model **a**, where **a** (**AA**) shows both type **A** for the ^{A}Se−H_b and ^{B}Se−$H_{b'}$ bonds in model **a**. Three conformers, **b** (**AA**-cis), **b** (**AB**), and **b** (**BB**), are stable for model **b**. The bonding models in **AA**, **AB**, and **BB** correspond to 3c−6e, 4c−6e, and 5c−6e, respectively. The models become more stable by 42 ± 5 kJ mol^{-1}, if the type **A** conformation of each Se−H bond changes to type **B**. No noticeable saturation is observed in the stabilization for each change. QC calculations are also performed on **1a**−**3a** at the B3LYP level. Three conformers are evaluated to be stable for **1a** and **2a**. The relative energies of **1a** (**AA**-trans), **1a** (**AB**), and **1a** (**BB**) are 0.0, −31.5, and −60.6 kJ mol^{-1}, respectively, and those of **2a** (**AA**-cis), **2a** (**AB**), and **2a** (**BB**) are 0.0, −24.4, and −36.5 kJ mol^{-1}, respectively. These results demonstrate that the origin of the linear alignment of the five C−Se- - -O- - -Se−C atoms in **1a** and **2a** is the energy lowering effect by the extended hypervalent 5c−6e interactions of the σ^*(C−Se)←n_p(O)→σ^*(Se−C) type. The π-conjugation between π(C=O) and n_{pz}(Se) through the π-framework of anthraquinone must also contribute to stabilize the **BB** structure of **1a**, where *z* is the direction perpendicular to the anthraquinone plane.

Introduction

Weak interactions are of current interest. van der Waals interactions are typical examples of weak interactions.[1] If nonbonded atoms in a molecule approach with each other closer than the sum of van der Waals radii of the atoms, orbitals at the atoms will directly overlap, which usually results in the large exchange repulsion. However, attractive interactions brought by the direct orbital overlaps can also be observed at distances less than the sum of van der Waals radii, if the exchange repulsion is suitably controlled. Naphthalene 1,8-positions supply a good system to study such phenomena,[2−6] since the nonbonded distances between atoms of main group elements at the 1,8-positions are close to the sum of van der Waals radii minus 1.0 Å. Various types of nonbonded interactions are expected for group 16 elements since they have both s- and p-type lone pair orbitals.[7] We have been highly interested in the nonbonded interactions that leads to linear bonds higher than the three center-four electron bonds (3c−4e). The extended hypervalent 4c−6e interactions of the linear four S and four Se atoms are investigated by the naphthalene system,[2a−f] together with the nonbonded 2c−4e and 3c−4e interactions.[2b,c,g,h] Anthracene 1,8,9-positions also serve as a good system for the interactions.[8]

* To whom correspondence should be addressed. Phone: +81-73-457-8252. Fax: +81-73-457-8253.

10.1021/jo035393+ CCC: $27.50
Published on Web 02/10/2004

To reveal the nature of 5c−6e is the next extension of our investigations on the extended hypervalent *m*c−*n*e ($m \geq 4$). 5c−6e are the σ-type linear bonds constructed by five atoms with six electrons, of which an approximate molecular model is shown in Scheme 1. How can 5c−6e be constructed? Our strategy is to employ the nonbonded interactions containing lone pairs. Lone-pair orbitals interact with others when they approach nearby and various types of charge-transfer (CT) will contribute to the nonbonded interactions containing lone pairs. Although the interactions are usually repulsive, they become attractive if all orbitals taking part in the interactions are not filled with electrons. CT from lone pairs to acceptors is accompanied by the attractive interactions. The driving force for the formation of X−Z−X 3c−4e is CT from the central atom Z to the outside atoms X, resulting in the highly polar $X^{\delta-}-Z^{\delta+}-X^{\delta-}$ bonds.[2c,9,10] That of X- - -Z-Z- - -X 4c−6e is CT from outside atoms X to the central σ^*(Z−Z), which forms polar $X^{\delta+}$- - -$Z^{\delta-}-Z^{\delta-}$- - -$X^{\delta+}$ bonds.[2a−f,11] The direction of CT in 4c−6e is just the opposite to that in 3c−4e. They are typical examples of the interactions. The bonds in Br_5^- and I_5^- are expected to be analyzed by the 5c−6e model, if the five atoms align linearly. Indeed, both linear[12a] and bent[12b] structures are reported for I_5^-, but the bent structures seem more stable than the linear ones for Br_5^- and I_5^- by QC calculations.[13] Environments of the anions must be important for the linear alignments. The infinite chain of $(O- - -Br-Br- - -)_n$ in an $Me_2CO- - -Br_2$ 1:1 complex[14] forms a long linear chain. However, the O- - -Br−Br- - -O bond in the adduct should be analyzed by the 4c−6e model,[13] since the infinite chain is bent at each oxygen atom with ∠BrOBr of 110°.

SCHEME 1. Approximate Molecular Orbital Model of Z_5 5c−6e

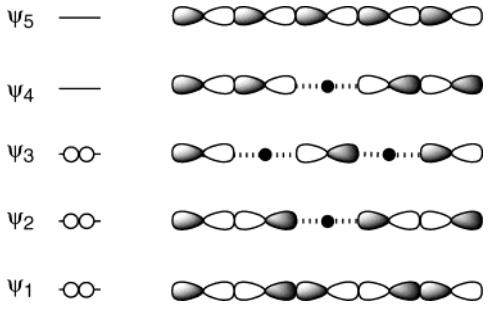

(1) (a) Scheiner, S., Ed. *Molecular Interactions. From van der Waals to Strongly Bound Complexes*, Wiley: New York, 1997. (b) Muller-Dethlefs, K.; Hobza, P. *Chem. Rev.* **2000**, *100*, 143−167. (c) Hobza, P.; Brutschy, B. *Chem. Rev.* **2000**, *100*, 3861−3862. Buck, U.; Huisken, F. *Chem. Rev.* **2000**, *100*, 3863−3890. Brutschy, B. *Chem. Rev.* **2000**, *100*, 3891−3920. Siglow, K.; Neusser, H. J. *Chem. Rev.* **2000**, *100*, 3921−3942. Desfrancois, C.; Carles, S.; Schermann, J. P. *Chem. Rev.* **2000**, *100*, 3943−3962. Biesuke, E. J.; Dopfer, O. *Chem. Rev.* **2000**, *100*, 3963−3998. Dessent, C. E. H.; Muller-Dethlefs, K. *Chem. Rev.* **2000**, *100*, 3999−4021. Dedonder-Lardeux, C.; Gregoire, G.; Jouvet, C.; Martrenchadd, S.; Solgadi, D. *Chem. Rev.* **2000**, *100*, 4023−4037. Zhong, Q.; Casrlrman, A. W., Jr. *Chem. Rev.* **2000**, *100*, 4039−4057. Niedner-Schatteburg, G.; Boddybey, V. E. *Chem. Rev.* **2000**, *100*, 4059−4086. Engkvist, O. *Chem. Rev.* **2000**, *100*, 4087−4108. Wormer, P. E. S.; van der Avoird, A. *Chem. Rev.* **2000**, *100*, 4109−4143. Kim, K. S.; Tarakeshwar, P.; Lee, J. Y. *Chem. Rev.* **2000**, *100*, 4145−4185. Orozco, M.; Luque, F. J. *Chem. Rev.* **2000**, *100*, 4187−4225. Chalasinski, G.; Szczesniak, M. M. *Chem. Rev.* **2000**, *100*, 4227−4252. Hobza, P.; Zdenek, H. *Chem. Rev.* **2000**, *100*, 4253−4264. See also: Hobza, P.; Selzle, H. L.; Schlag, E. W. *Chem. Rev.* **1994**, *94*, 1767−1785. Reed, A. E.; Curtiss, L. A.; Weinhold, F. *Chem. Rev.* **1988**, *88*, 899−926.

(2) (a) Nakanishi, W.; Hayashi, S.; Toyota, S. *Chem. Commun.* **1996**, 371−372. (b) Nakanishi, W.; Hayashi, S.; Toyota, S. *J. Org. Chem.* **1998**, *63*, 8790−8800. (c) Nakanishi, W.; Hayashi, S.; Yamaguchi, H. *Chem. Lett.* **1996**, 947−948. (d) Hayashi, S.; Nakanishi, W. *J. Org. Chem.* **1999**, *64*, 6688−6696. (e) Nakanishi, W.; Hayashi, S. *J. Org. Chem.* **2002**, *67*, 38−48. (f) Nakanishi, W.; Hayashi, S.; Arai, T. *Chem. Commun.* **2002**, 2416−2417. (g) Nakanishi, W.; Hayashi, S.; Uehara, T. *J. Phys. Chem. A* **1999**, *103*, 9906−9912. (h) Nakanishi, W.; Hayashi, S.; Sakaue, A.; Ono, G.; Kawada, Y. *J. Am. Chem. Soc.* **1998**, *120*, 3635−3646.

(3) (a) Glass, R. S.; Andruski, S. W.; Broeker, J. L. Rev. *Heteroatom Chem.* **1988**, *1*, 31−45. (b) Glass, R. S.; Andruski, S. W.; Broeker, J. L.; Firouzabadi, H.; Steffen, L. K.; Wilson, G. S. *J. Am. Chem. Soc.* **1989**, *111*, 4036−4045. (c) Glass, R. S.; Adamowicz, L.; Broeker, J. L. *J. Am. Chem. Soc.* **1991**, *113*, 1065−1072.

(4) (a) Mallory, F. B. *J. Am. Chem. Soc.* **1973**, *95*, 7747−7752. (b) Mallory, F. B.; Mallory, C. W.; Fedarko, M.-C. *J. Am. Chem. Soc.* **1974**, *96*, 3536−3542. (c) Mallory, F. B.; Mallory, C. W.; Ricker, W. M. *J. Am. Chem. Soc.* **1975**, *97*, 4770−4771. Mallory, F. B.; Mallory, C. W.; Ricker, W. M. *J. Org. Chem.* **1985**, *50*, 457−461. Mallory, F. B.; Mallory, C. W.; Baker, M. B. *J. Am. Chem. Soc.* **1990**, *112*, 2577−2581. (d) Mallory, F. B.; Mallory, C. W.; Butler, K. B.; Lewis, M. B.; Xia, A. Q.; Luzik, E. D., Jr.; Fredenburgh, L. E.; Ramanjulu, M. M.; Van, Q. N.; Francl, M. M.; Freed, D. A.; Wray, C. C.; Hann, C.; Nerz-Stormes, M.; Carroll, P. J.; Chirlian, L. E. *J. Am. Chem. Soc.* **2000**, *122*, 4108−4116. (e) Mallory, F. B.; Luzik, E. D., Jr.; Mallory, C. W.; Carroll, P. J. *J. Org. Chem.* **1992**, *57*, 366−370. Mallory, F. B.; Mallory, C. W. *J. Am. Chem. Soc.* **1985**, *107*, 4816−4819.

(5) (a) Fujihara, H.; Ishitani, H.; Takaguchi, Y.; Furukawa, N. *Chem. Lett.* **1995**, 571−572. Fujihara, H.; Yabe, M.; Chiu, J.-J.; Furukawa, N. *Tetrahedron Lett.* **1991**, *32*, 4345−4348. Furukawa, N.; Fujii, T.; Kimura, T.; Fujihara, H. *Chem. Lett.* **1994**, 1007−1010. Fujihara, H.; Saito, R.; Yabe, M.; Furukawa, N. *Chem. Lett.* **1992**, 1437−1440. Johannsen, I.; Eggert, H. *J. Am. Chem. Soc.* **1984**, *106*, 1240. Johannsen, I.; Eggert, H.; Gronowitz, S.; Hörnfeldt, A.-B. *Chem. Scr.* **1987**, *27*, 359−361. Fujihara, H.; Mima, H.; Erata, T.; Furukawa, N. *J. Am. Chem. Soc.* **1992**, *114*, 3117−3118.

(6) Gafner, G.; Herbstein, F. H. *Acta Crystallogr.* **1962**, *15*, 1081−1092. Davydova, M. A.; Struchkov, Yu. T. *Zh. Strukt. Kim.* **1962**, *3*, 184−199. Davydova, M. A.; Struchkov, Yu. T. *Zh. Strukt. Khim.* **1968**, *9*, 258−266. Bock, H.; Sievert, M.; Havlas, Z. *Chem.-A Eur. J.* **1998**, *4*, 677−685. Jackson, R. D.; James, S.; Orpen, A. G.; Pringle, P. G. *J. Organomet. Chem.* **1993**, *458*, C3−C4. Schweizer, W. B.; Procter, G.; Kaftory, M.; Dunitz, J. D. *Helv. Chim. Acta* **1978**, *61*, 2783−2808. Procter, G.; Britton, D.; Dunitz, J. D. *Helv. Chim. Acta* **1981**, *64*, 471−477. Mugesh, G.; Singh, H. B. *Acc. Chem. Rev.* **2002**, *35*, 226−236.

(7) (a) Asmus, K. D. *Acc. Chem. Res.* **1979**, *12*, 436−442. (b) Musker, W. K. *Acc. Chem. Res.* **1980**, *13*, 200−206. (c) Kucsman, A.; Kapovits, I. In *Nonbonded Sulfur−oxygen Interaction in Organic Sulfur Compounds in Organic Sulfur Chemistry: Theoretical and Experimental Advances*; Bernardi, F., Csizmadia, I. G., Mangini, A., Eds.; Elsevier: Amsterdam, 1985.

(8) (a) Akiba, K.-y.; Yamashita, M.; Yamamoto, Y.; Nagase, S. *J. Am. Chem. Soc.* **1999**, *121*, 10644−10645. (b) Yamashita, M.; Yamamoto, Y.; Akiba, K.-y.; Nagase, S. *Angew. Chem., Int. Ed.* **2000**, *39*, 4055−4058. Yamashita, M.; Watanabe, K.; Yamamoto, Y.; Akiba, K.-y. *Chem. Lett.* **2001**, 1104−1105.

(9) (a) Pimentel, G. C. *J. Chem. Phys.* **1951**, *19*, 446−448. Musher, J. I. *Angew. Chem., Int. Ed. Engl.* **1969**, *8*, 54−68. Chen, M. M. L.; Hoffmann, R. *J. Am. Chem. Soc.* **1976**, *98*, 1647−1653. Cahill, P. A.; Dykstra, C. E.; Martin, J. C. *J. Am. Chem. Soc.* **1985**, *107*, 6359−6362. (b) Baenziger, N. C.; Buckles, R. E.; Maner, R. J.; Simpson, T. D. *J. Am. Chem. Soc.* **1969**, *91*, 5749−5755.

(10) Klayman, D. L.; Günther, W. H. H. *Organic Selenium Compounds: Their Chemistry and Biology*; Wiley: New York, 1973; Chapter XV. Perkins, C. W.; Martin, J. C.; Arduengo, A. J.; Lau, W.; Alegria, A.; Kochi, J. K. *J. Am. Chem. Soc.* **1980**, *102*, 7753−7759. Hayes, R. A.; Martin, J. C. In *Sulfurane Chemistry in Organic Sulfur Chemistry: Theoretical and Experimental Advances*; Bernardi, F., Csizmadia, I. G., Mangini, A., Eds.; Elsevier: Amsterdam, 1985 and references cited therein. Akiba, K.-y. *Chemistry of Hypervalent Compounds*; Wiley-VCH: New York, 1999 and references cited therein.

(11) Alvarez, S.; Mota, F.; Novoa, J. *J. Am. Chem. Soc.* **1987**, *109*, 6586−6591. Siepmann, R.; von Schnering, H. G. *Z. Anorg. Allg. Chem.* **1968**, *357*, 289−298.

(12) (a) Akutagawa, T.; Abe, Y.; Nezu, Y.; Nakamura, T.; Kataoka, M.; Yamanaka, A.; Inoue, K.; Inabe, T.; Christensen, C. A.; Becher, J. *Inorg. Chem.* **1998**, *37*, 2330−2331. Starodub, V. A.; Baumer, V. N.; Guella, I. M.; Golovkina, I. F.; Alyoshin, V. G.; Nemoshkalenko, V. V.; Senkiewicz, A. I. *Synthetic Metals* **1983**, *5*, 101−111. (b) Svensson, P. H.; Kloo, L. *J. Chem. Soc., Dalton Trans.* **2000**, 2449−2455. Tebbe, K.-F.; Loukili, R. *Z. Anorg. Allg. Chem.* **1999**, *625*, 820−826.

(13) Nakanishi, W. Unpublished results.

(14) Hassel, O.; Stromme, K. O. *Acta. Chem. Scand.* **1959**, *13*, 275−280.

CHART 1

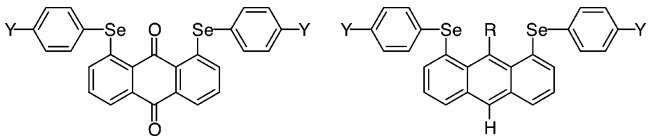

1a (Y = H)
1b (Y = Cl)

2a (R = OMe, Y = H)
3a (R = H, Y = H)
3b (R = H, Y = Cl)

Here, we report the linear alignment of five C_i−Se- - -O- - -Se−C_i atoms in 1,8-bis(arylselanyl)anthraquinones [1,8-(p-$YC_6H_4Se)_2C_{14}H_6O_2$: **1a** (Y = H) and **1b** (Y = Cl)] and 1,8-bis(phenylselanyl)-9-methoxyanthracene [1,8-$(C_6H_5Se)_2$-9-$MeOC_{14}H_7$: **2a**] (Chart 1).[15] The linear alignment is analyzed by the 5c−6e model of the $\sigma^*(C_i-Se)$- - -$n_p(O)$- - -$\sigma^*(Se-C_i)$ type based on QC calculations. The structures of 1,8-bis(arylselanyl)anthracenes [1,8-(p-$YC_6H_4Se)_2C_{14}H_8$: **3a** (Y = H) and **3b** (Y = Cl)] (Chart 1) are also investigated for convenience of comparison. However, the five C_i−Se- - -H- - -Se−C_i atoms in **3a** and **3b** never align linearly.

Results

X-ray Crystallographic Analysis. Single crystals of **1a**,**b**, **2a**, and **3a**,**b** were obtained via slow evaporation of benzene solutions containing 10−30 v/v% of ethanol. X-ray crystallographic analysis was carried out for the suitable single crystals. Only one type of structure corresponds to each compound in the crystals. Crystallographic data, together with the selected interatomic distances, angles, and torsional angles, are collected in the Supporting Information.[16] Figures 1−3 show the structures of **1a**−**3a**, respectively. Structures of **1b** and **3b** are shown in the Supporting Information.[16]

QC Calculations. To reveal the nature of 5c−6e in **1** and **2**, QC calculations are performed on model **a** and model **b** and the real system, **1a**−**3a**.

Model Calculations. Model **a** ($H_aH_b{}^ASe$- - -O(=CH_2)- - -$^BSeH_{a'}H_{b'}$) and model **b** ($H_aH_b{}^ASe$- - -OH_2- - -$^BSeH_{a'}H_{b'}$) are devised based on the structures of **1** and **2**, respectively (Chart 2). QC calculations are performed on the models, using the Gaussian 94[17] and/or 98[18] programs with the B3LYP/6-311++G(3df,2pd) method.

The O atom of model **a** is placed at the origin, the O=C bond on the y-axis, and two H atoms on the xy plane. Two Se atoms are located on the x-axis of the opposite side. Nonbonded Se- - -O distances are fixed at $r(^ASe,O) = r(^BSe,O) = 2.658$ Å.[19] The $^ASe-H_a$ and $^BSe-H_{a'}$ bonds are placed on the y direction. Consequently, eight atoms are placed on the xy plane. Valuables are optimized for r(C,O), r(C,H) ∠OCH, r(Se,H), $\angle H_a{}^ASeH_b$ (= θ_A), $\angle H_{a'}{}^BSeH_{b'}$ (= θ_B), and torsional angles of OH_a-$^ASeH_b$ (= ϕ_A) and $OH_{a'}{}^BSeH_{b'}$ (= ϕ_B). Four conformers, **a** (**AA**-cis), **a** (**AA**-trans), **a** (**AB**), and **a** (**BB**), are optimized to be stable, where **a** (**AA**) shows the type **A**-type **A** pairing for $^ASe-H_b$ and $^BSe-H_{b'}$ in model **a**, for an example.[20] Conformers, **a** (**AA**-trans), **a** (**AB**), and **a** (**BB**), are more stable than **a** (**AA**-cis) by 0.5, 45.7, and 87.4 kJ mol^{-1}, respectively. Figure 4 exhibits the stable conformers of model **a**, together with the relative energies.[21]

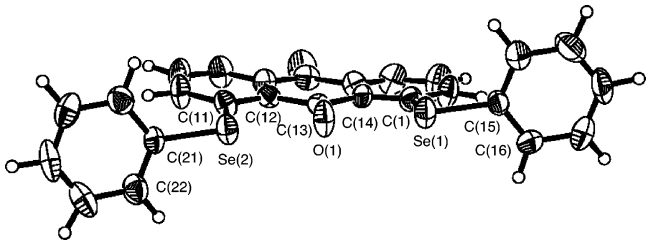

FIGURE 1. Structure of **1a**. Selected bond lengths (Å), angles (deg), and torsion angles (deg): Se(1)−C(1), 1.922(7); Se(1)−C(15), 1.924(6); Se(2)−C(11), 1.917(6); Se(2)−C(21), 1.927(6); C(13)−O(1), 1.225(7); Se(1)−O(1), 2.688(4), Se(2)−O(1), 2.673(4); C(1)−Se(1)−C(15), 98.5(3); C(11)−Se(2)−C(21), 100.2(3); Se(1)−O(1)−Se(2), 152.5(2); C(14)−C(1)−Se(1)−C(15), −172.8(6); C(12)−C(11)−Se(2)−C(21), −171.3(5); C(1)−Se(1)−C(15)−C(16), 90.5(6); C(11)−Se(2)−C(21)−C(22), 103.5(6). Thermal ellipsoids drawn at 50% probability level.

Similarly, the O atom of model **b** is placed at the origin and the O−^{1}H bond on the y-axis. Two Se atoms are located on the x-axis of the opposite side. Nonbonded Se- - -O distances are fixed at the $r(^ASe,O) = r(^BSe,O) = 2.658$ Å.[19] The $^ASe-H_a$ and $^BSe-H_{a'}$ bonds are placed on the y direction. Therefore, six atoms are placed on the xy plane. Valuables are optimized for r(O,H), ∠HOH, r(Se,H), $\angle H_a{}^ASeH_b$ (= θ_A), $\angle H_{a'}{}^BSeH_{b'}$ (= θ_B), and torsional angles of $^ASe^1HO^2H$ (= ϕ_O), $OH_a{}^ASeH_b$ (= ϕ_A), and $OH_{a'}{}^BSeH_{b'}$ (= ϕ_B). Three conformers, **b** (**AA**-cis), **b** (**AB**), and **b** (**BB**), are optimized to be stable for model **b**:[22] The relative energies are 0.0, −45.4, and −82.7 kJ mol^{-1},

(15) Preliminary communication: Nakanishi, W.; Hayashi, S.; Itoh, N. *Chem. Commun.* **2003**, 124−125.

(16) Crystallographic data for **1a**,**b**, **2a**, and **3a**,**b** are shown in Table S1 and the structures of **1b** and **3b** are shown in Figures S1 and S2, respectively, in the Supporting Information. The structures of **1b** and **3b** are substantially the same as those of **1a** and **3a**, respectively.

(17) Gaussian 94, Revision D.4: Frisch, M. J.; Trucks, G. W.; Schlegel, H. B.; Gill, P. M. W.; Johnson, B. G.; Robb, M. A.; Cheeseman, J. R.; Keith, T.; Petersson, G. A.; Montgomery, J. A.; Raghavachari, K.; Al-Laham, M. A.; Zakrzewski, V. G.; Ortiz, J. V.; Foresman, J. B.; Cioslowski, J.; Stefanov, B. B.; Nanayakkara, A.; Challacombe, M.; Peng, C. Y.; Ayala, P. Y.; Chen, W.; Wong, M. W.; Andres, J. L.; Replogle, E. S.; Gomperts, R.; Martin, R. L.; Fox, D. J.; Binkley, J. S.; Defrees, D. J.; Baker, J.; Stewart, J. P.; Head-Gordon, M.; Gonzalez, C.; Pople, J. A. Gaussian, Inc., Pittsburgh, PA, 1995.

(18) Gaussian 98, Revision A.9: Frisch, M. J.; Trucks, G. W.; Schlegel, H. B.; Scuseria, G. E.; Robb, M. A.; Cheeseman, J. R.; Zakrzewski, V. G.; Montgomery, J. A., Jr.; Stratmann, R. E.; Burant, J. C.; Dapprich, S.; Millam, J. M.; Daniels, A. D.; Kudin, K. N.; Strain, M. C.; Farkas, O.; Tomasi, J.; Barone, V.; Cossi, M.; Cammi, R.; Mennucci, B.; Pomelli, C.; Adamo, C.; Clifford, S.; Ochterski, J.; Petersson, G. A.; Ayala, P. Y.; Cui, Q.; Morokuma, K.; Malick, D. K.; Rabuck, A. D.; Raghavachari, K.; Foresman, J. B.; Cioslowski, J.; Ortiz, J. V.; Baboul, A. G.; Stefanov, B. B.; Liu, G.; Liashenko, A.; Piskorz, P.; Komaromi, I.; Gomperts, R.; Martin, R. L.; Fox, D. J.; Keith, T.; Al-Laham, M. A.; Peng, C. Y.; Nanayakkara, A.; Challacombe, M.; Gill, P. M. W.; Johnson, B.; Chen, W.; Wong, M. W.; Andres, J. L.; Gonzalez, C.; Head-Gordon, M.; Replogle, E. S.; Pople, J. A. Gaussian, Inc., Pittsburgh, PA, 1998.

(19) The fixed value of 2.658 Å is obtained by averaging the observed values for 1,8-bis(p-chlorophenylselanyl)anthraquinone (**1b**). The value is slightly different from that in the Supporting Information. A revised value is given in the Supporting Information where the accuracy of the measurement have been improved.

(20) Structures of the naphthalene system, 8-G-1-(ArSe)$C_{10}H_6$, are well classified using type **A**, type **B**, and type **C**, where the Se−C_{Ar} bond is placed almost perpendicular to the naphthyl plane in type **A**, the bond is located on the plane in type **B**, and the type **C** structure is the intermediate between type **A** and type **B**. See ref 2 and: Nakanishi, W.; Hayashi, S. *Eur. J. Org. Chem.* **2001**, 3933−3943.

(21) The optimized structures and the calculated natural charges (Qn) of model **a** and model **b**, together with the components, are given in Tables S2 and S3, respectively, in the Supporting Information.

(22) The conformer **b** (**AA**-trans) converges to **b** (**AB**), if the calculations are started with the C_1 symmetry.

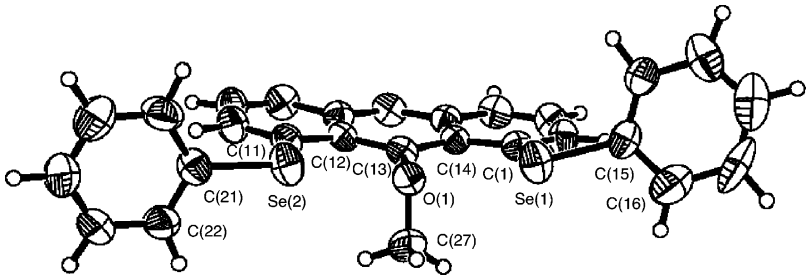

FIGURE 2. Structure of **2a**. Selected bond lengths (Å), angles (deg), and torsion angles (deg): Se(1)−C(1), 1.930(4); Se(1)−C(15), 1.921(5); Se(2)−C(11), 1.932(5); Se(2)−C(21), 1.938(5); C(13)−O, 1.387(5); C(27)−O, 1.436(6); Se(1)−O, 2.731(3); Se(2)−O, 2.744(3); C(1)−Se(1)−C(15), 99.2(2); C(11)−Se(2)−C(21), 99.9(2); C(13)−O−C(27), 111.7(4); Se(1)−O−Se(2), 147.9(1); C(14)−C(1)−Se(1)−C(15), −163.1(4); C(12)−C(11)−Se(2)−C(21), 175.8(4); C(1)−Se(1)−C(15)−C(16), −104.2(5); C(11)−Se(2)−C(21)−C(22), 88.3(5); C(14)−C(13)−O−C(27), 89.1(5). Thermal ellipsoids drawn at 50% probability level.

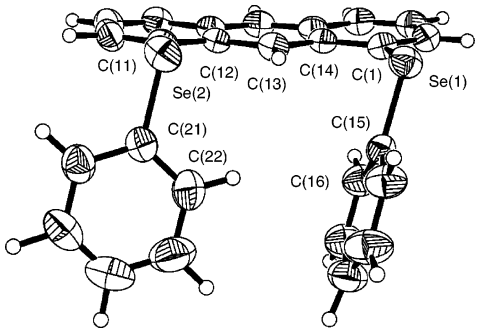

FIGURE 3. Structure of **3a**. Selected bond lengths (Å), angles (deg), and torsion angles (deg): Se(1)−C(1), 1.923(3); Se(1)−C(15), 1.923(3); Se(2)−C(11), 1.943(3); Se(2)−C(21), 1.931(3); C(1)−Se(1)−C(15), 100.3(1); C(11)−Se(2)−C(21), 98.3(1); C(14)−C(1)−Se(1)−C(15), 72.6(3); C(12)−C(11)−Se(2)−C(21), −103.0-(3); C(1)−Se(1)−C(15)−C(16), 6.7(3); C(11)−Se(2)−C(21)−C(22), 85.8(3). Thermal ellipsoids drawn at 50% probability level.

CHART 2 Model a and Model b

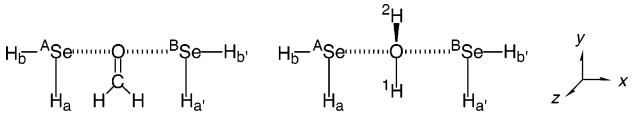

respectively. Figure 4 exhibits the stable conformers of model **b**, together with the relative energies.[21]

Natural charges (*Qn*) are also calculated for the stable conformers of the models shown in Figure 4, together with the components, SeH_2, $O{=}CH_2$, and OH_2, by the natural population analysis of the Gaussian program.[23] Table 1 shows the *Qn* values for the SeH_2, $O{=}CH_2$, and OH_2 molecules in the stable conformers of model **a** and model **b**. Details of the calculations are shown in the Supporting Information.[21]

How do the energies of model **a** and model **b** correlate with the structures? The angular dependence of the energy *E* of model **a** is calculated with variously fixed ϕ_A (ϕ for $OH_a{}^ASeH_b$) in a range of 45° ≤ ϕ_A ≤ 315°. The conformations around ^{A}Se are type **A**, type **B**, and type **A** when the ϕ_A value is given nearly 90°, 180°, and 270°, respectively. Energies (E_1 and E_2) and angles (ϕ_{B1} and ϕ_{B2}) are obtained in the optimization for each fixed value

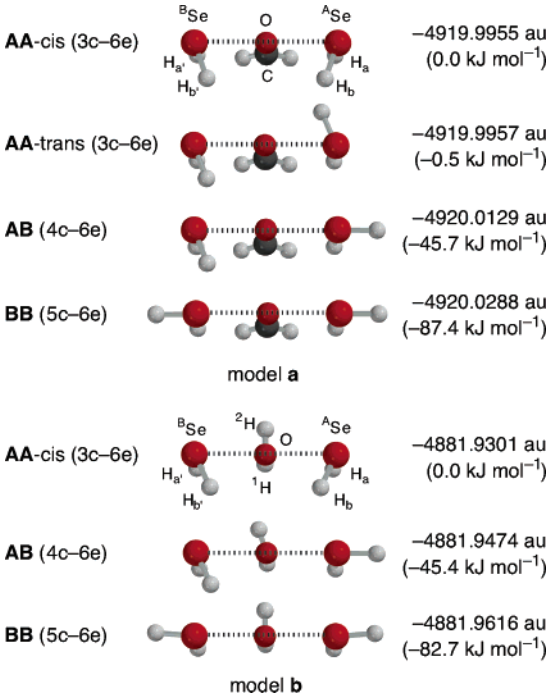

FIGURE 4. Stable conformers and the energies for model **a** and model **b**, calculated with the B3LYP/6-311++G(3df,2pd) method.

of ϕ_A: E_1 and E_2 correspond to the structures with ϕ_{B1} and ϕ_{B2}, respectively. The ϕ_{B1} and ϕ_{B2} values are nearly 90° and/or 180°, respectively: ϕ_{B1} and ϕ_{B2} are almost maintained at the values even when the fixed value of ϕ_A is changed. This means that the conformation around the ^{B}Se atom is stable when it is type **A** or type **B**. Figure 5 shows the results, that explain well the energy profile of model **a**.

Molecular orbitals are drawn for the optimized structures of **a** (**BB**) and **b** (**BB**) given in Figure 4. Single point calculations are performed using the MacSpartan Plus program[24] with the 3-21G basis sets. Figure 6 shows some MOs of **a** (**BB**) and **b** (**BB**), which correspond to ψ_1, ψ_3, and ψ_4 of HSeOSeH 5c−6e. Figure 6 also contains an approximate molecular orbital model of 5c−6e of the linear five H−Se- - -O- - -Se−H atoms.

QC Calculations on 1a−3a. QC calculations are performed on **1a**−**3a**, with the B3LYP/Gen method

(23) Glendening, E. D.; Reed, A. E.; Carpenter, J. E.; Weinhold, F. NBO Ver. 3.1, equipped in Gaussian programs.

(24) MacSpartan Plus program Ver. 1.0 is used, Hehre, H. J. Wavefunction Inc., Irvin, CA 92612.

TABLE 1. *Qn* Values for the SeH_2, OCH_2, and OH_2 Molecules in Model a and Model b, Calculated with the B3LYP/6-311++G(3df,2pd) Method

	model **a**				model **b**		
	$Qn(^{A}SeH_2)$	$Qn(^{B}SeH_2)$	$Qn(OCH_2)$		$Qn(^{A}SeH_2)$	$Qn(^{B}SeH_2)$	$Qn(H_2O)$
a (**AA**-cis)	0.0094	0.0094	−0.0188	**b** (**AA**-cis)	−0.0008	−0.0008	0.0016
a (**AA**-trans)	0.0093	0.0093	−0.0186				
a (**BA**)	−0.0225	0.0135	0.0090	**b** (**BA**)	−0.0345	0.0059	0.0283
a (**BB**)	−0.0170	−0.0170	0.0340	**b** (**BB**)	−0.0285	−0.0285	0.0570

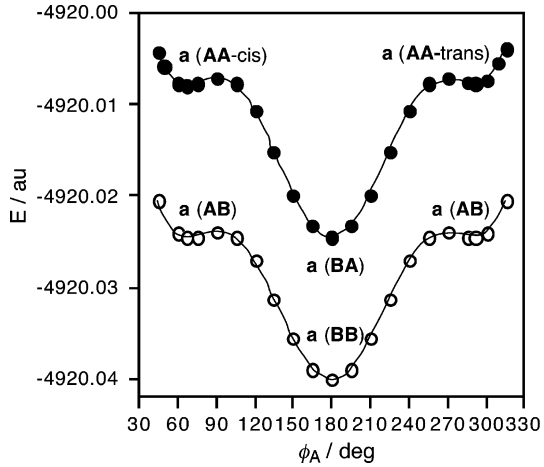

FIGURE 5. Torsional angular (ϕ_A: $OH_a{}^{A}SeH_b$) dependence of energy in model **a**, calculated with the B3LYP/6-311++G(3df,2pd) method.

(6-311+G(d) basis sets being employed for Se and O and 6-31G(d) basis sets for C and H at the B3LYP level). The results are collected in Table 2. Three conformers around the two Se atoms, type **A**−type **A**, type **A**−type **B**, and type **B**−type **B** pairings, are essentially optimized to be stable for the three compounds: Only the trans conformer of type **A**−type **A** is optimized for **1a**, only the cis conformer for **2a**, and both the cis and trans conformers for **3a**. The conformers are named **na** (**AA**-cis) (and/or **na** (**AA**-trans)), **na** (**AB**), **na** (**BB**), respectively, where **n** = **1**−**3**. While the observed structures are well reproduced to be most stable for **1a** and **2a** by the calculations, the observed **3a** (**AA**-cis) is predicted to be slightly less stable than **3a** (**AA**-trans) and **3a** (**AB**). Figure 7 shows the results.

Molecular orbitals are also drawn[24] for the optimized structures of **1a** (**BB**), **2a** (**BB**), and **3a** (**AA**-cis). Figure 8 shows some MOs: HOMO-2 of **1a**, HOMO-9 of **2a**, and HOMO-1 and HOMO-3 of **3a**. The MOs are extended over the linear five C−Se- - -O- - -Se−C atoms in **1a** and **2a**, but they are mainly localized on each Se atom or PhSe group in **3a**.

Discussion

Structures of 1−3. The structure of **1a** is close to the C_2 symmetry and the conformations around the two Se atoms are both type **B** (Figure 1):[20] The torsional angles of C(14)C(1)Se(1)C(15) and C(12)C(11)Se(2)C(21) are −172.8(6)° and −171.3(5)°, respectively. Two phenyl planes are perpendicular to the anthraquinone plane. Consequently, the five C_i−Se- - -O- - -Se−C_i atoms align linearly with ∠Se(1)O(1)Se(2) = 152.5(2)°. The slight bend structure of the alignment is a reflection mainly of the differences among *r*(C(13)−O(1)), *r*(C(1)−Se(1)), and *r*(C(11)−Se(2)), although the structure is also affected by the angles around the atoms. The structure of **1b**, shown in the Supporting Information, is very close to that of **1a**.

The structure of **2a**, bearing an MeO group at the 9-position, is close to the C_s symmetry with the conformations around the two Se atoms being both type **B** (Figure 2):[20] The torsional angles of C(14)C(1)Se(1)C(15) and C(12)C(11)Se(2)C(21) are −163.1(4)° and 175.8(4)°, respectively. Two phenyl planes are perpendicular to the anthracene plane. The five C_i−Se- - -O- - -Se−C_i atoms in **2a** also align almost linearly with ∠Se(1)O(1)Se(2) = 147.9(1)°, which is also mainly the results from the differences among *r*(C(13)−O(1)), *r*(C(1)−Se(1)), and *r*(C(11)−Se(2)). The smaller value of ∠Se(1)O(1)Se(2) in **2a** relative to **1a** must come from the differences in the angles around the atoms since *r*(C(13)−O(1)) of **2a** is larger than that of **1a**. Indeed, the structure of **2a** is very similar to that of **1a**, but the Me group in **2a** makes it close to the C_s symmetry contrary to the C_2 like one in **1a**.

On the other hand, the structure of **3a** is very different from those of **1a** and **2a** (Figure 3). The conformations around the Se atoms in **3a** are both type **A**,[20] and two phenyl groups are located at the same side of the plane (cis-conformation): ∠C(14)C(1)Se(1)C(15) = 72.6(3)° and ∠C(12)C(11)Se(2)C(21) = −103.0(3)°. The conformations of the phenyl groups around the Se−C_i bonds are characteristic. The phenyl planes are nearly perpendicular with each other: The Se(1)−C(1) bond is on the Ph plane bearing the *ipso* C(15) carbon but the Se(2)−C(11) bond is perpendicular to that with the *ipso* C(21) carbon. The five C_i−Se- - -H- - -Se−C_i atoms in **3a** never align linearly. The structure of **3b**, shown in the Supporting Information, is also very close to that of **3a**. One easily realizes that the double type **A** structure of **3** dramatically changes to the double type **B** structures in **1** and **2** by the oxygen atom at the 9-position of each compound.

The nonbonded Se- - -O distances in **1a**, **1b**, and **2a** are 2.673−2.688, 2.643−2.662, and 2.731−2.744 Å, respectively, which are 0.66−0.76 Å shorter than the sum of the van der Waals radii of the atoms (3.40 Å).[25] Such shorter nonbonded Se- - -O distances result in the direct orbital overlaps between those at the atoms. The extension of the n_p(O) orbital toward σ^*(Se−C) orbitals must be most important to determine the structures of **1** and **2** among a lot of nonbonded orbital interactions. If hypervalent n_p(O)- - -σ^*(Se−C) 3c−4e type interactions occur toward both side of the central n_p(O) orbital, and if they are connected by the common n_p(O) orbital, the resulting σ^*(C−Se)- - -n_p(O)- - -σ^*(Se−C) interaction can

(25) Pauling, L. *The Nature of the Chemical Bond*, 3rd ed.; Cornell University Press: Ithaca, NY, 1960; Chapter 7.

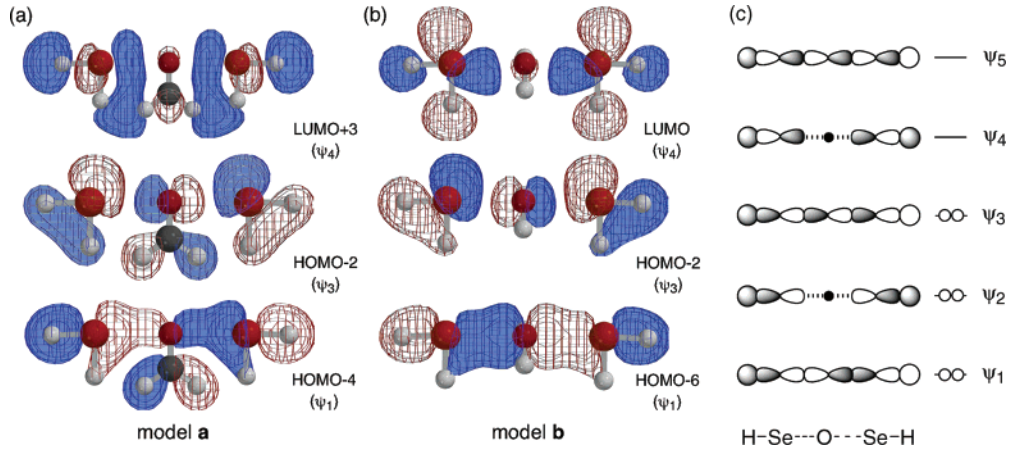

FIGURE 6. Molecular orbitals for linear five H−Se- - -O- - -Se−H atoms: (a) HOMO-4 (ψ_1), HOMO-2 (ψ_3), LUMO+3 (ψ_4) of model **a**, and (b) HOMO-6 (ψ_1), HOMO-2 (ψ_3), and LUMO (ψ_4) of model **b**, and (c) approximate molecular orbital model of HSeOSeH 5c−6e.

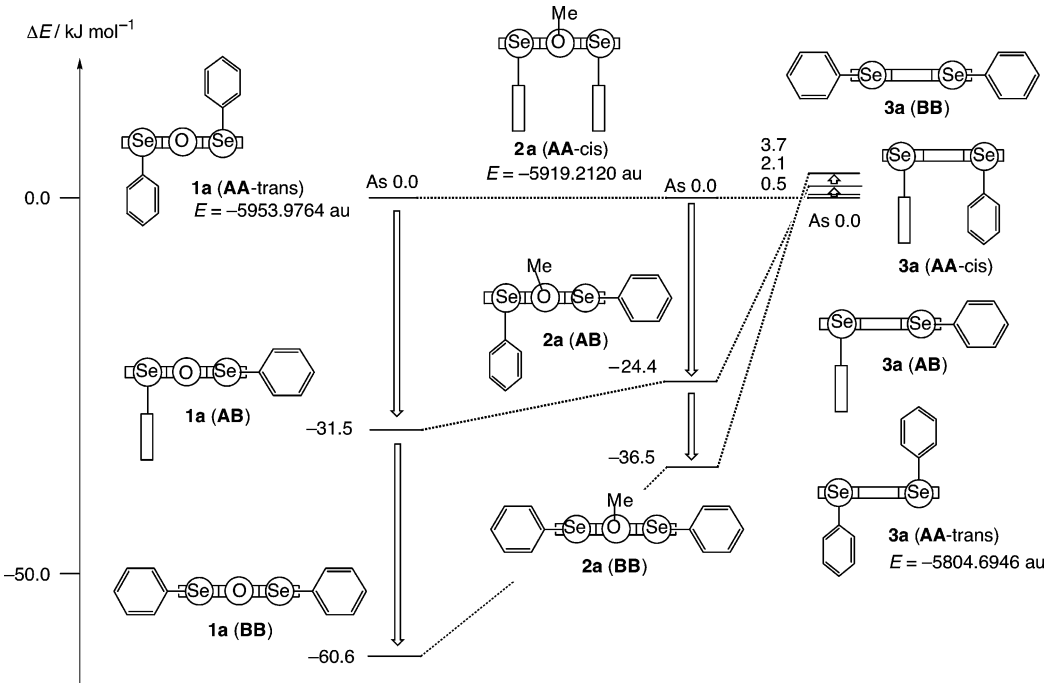

FIGURE 7. Stable conformers and relative energies for **1a**, **2a**, and **3a**, calculated with the B3LYP/Gen method: 6-311+G(d) basis sets were employed for Se and O and 6-31G(d) for C and H.

TABLE 2. Energies of Various Conformers in 1a, 2a, and 3a, Calculated with the B3LYP/Gen Method: 6-311+G(d) Basis Sets Employed for Se and O and 6-31G(d) Basis Sets for C and H

	1a		**2a**		**3a**	
conformation	*E*/au (Δ*E*/kJ mol^{-1})		*E*/au (Δ*E*/kJ mol^{-1})		*E*/au (Δ*E*/kJ mol^{-1})	
AA-trans	−5953.9764	(0.0)			−5804.6946	(0.0)
AA-cis			−5919.2120	(0.0)	−5804.6938	(2.1)
AB	−5953.9884	(−31.5)	−5919.2213	(−24.4)	−5804.6944	(0.5)
BB	−5953.9995	(−60.6)	−5919.2259	(−36.5)	−5804.6932	(3.7)

be totally analyzed by the 5c−6e model. Consequently, the linear alignment of five C−Se- - -O- - -Se−C atoms in **1** and **2** is well explained by the extended hypervalent 5c−6e interaction.

Extended Hypervalent HSeOSeH 5c−6e in Models. The optimized structures for model **a** and model **b** are shown in Figure 4. Four conformers, **a** (**AA**-cis), **a** (**AA**-trans), **a** (**AB**), and **a** (**BB**), are optimized to be stable for model **a**: **a** (**AA**-trans), **a** (**AB**), and **a** (**BB**) are more stable than **a** (**AA**-cis) by 0.5, 45.7, and 87.4 kJ mol^{-1}, respectively. On the other hand, three conformers, **b** (**AA**-cis), **b** (**AB**), and **b** (**BB**), are stable in model **b**: **b** (**AB**) and **b** (**BB**) are more stable than **b** (**AA**-cis) by 45.4 and 82.7 kJ mol^{-1}, respectively.[22] The characters of interactions in **AA**, **AB**, and **BB** of the models are 3c−6e,[26] 4c−6e, and 5c−6e, respectively. The conformers become more

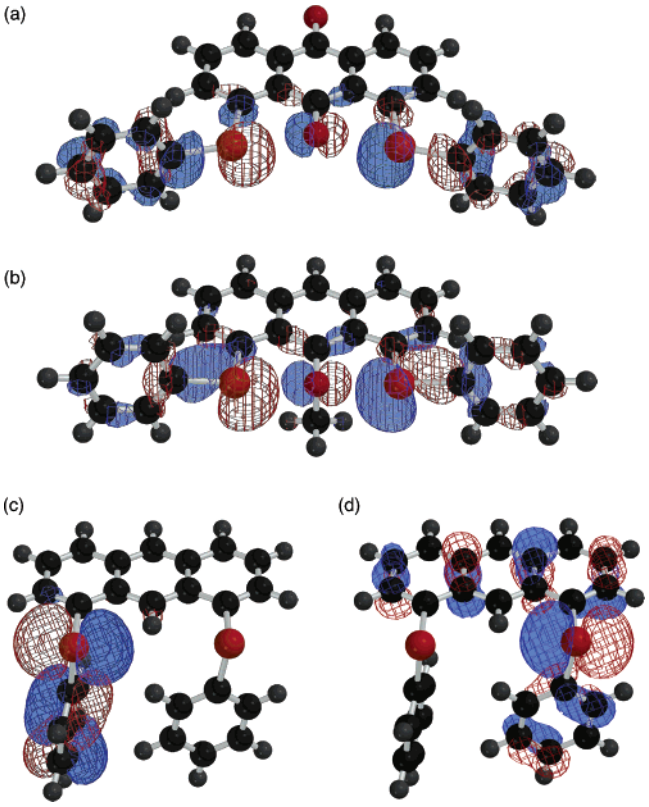

FIGURE 8. Some molecular orbitals of **1a**, **2a**, and **3a**: (a) HOMO-2 of **1a**, (b) HOMO-9 of **2a**, (c) HOMO-1 of **3a**, and (d) HOMO-3 of **3a**.

stable by 42 ± 5 kJ mol^{-1}, if the type **A** conformer of each Se−H changes to type **B**, irrespective of the different central groups of H_2C═O and H_2O.[27] No noticeable saturation is observed in the stabilization for the conformational changes. The results show that two hypervalent n_{px}(O)- - -σ*(Se−H) 3c−4e interactions operate effectively together in σ*(H−Se)- - -n_{px}(O)- - -σ*(Se−H) through the central n_{px}(O) orbital in the models, which must be the nature of the extended hypervalent 5c−6e interactions.

The energy profile of model **a** clarifies the nature of the extended hypervalent H−Se- - -O- - -Se−H 5c−6e interaction (Figure 5). The conformation around ^{A}Se is determined by the fixed value of ϕ_A. The optimization with a fixed ϕ_A yields two different energies E (E_1 and E_2) and angles ϕ_B (ϕ_{B1} and ϕ_{B2}): E_1 and E_2 correspond to the structures with ϕ_{B1} and ϕ_{B2}, respectively. The conformations around the ^{B}Se atom are determined by ϕ_{B1} and ϕ_{B2}, respectively. The conformers are type **A** or type **B**, since ϕ_{B1} and ϕ_{B2} are predicted to be close to 90°or 180°. Conformers of **a** (**AA**-cis), **a** (**BA**), and **a** (**AA**-trans) are on an E_1 curve and those of **a** (**AB**), **a** (**BB**), and **a** (**AB**) are on an E_2 curve. Figure 5 tells that (1) the conformation around ^{B}Se maintained nearly 90° or 180° under the calculated conditions when energy sweep is carried out with the variously fixed ϕ_A and (2) the conformation around ^{A}Se well controls that of ^{B}Se. The two curves are almost coincident with each other, which shows that the saturation of the energy lowering effect is negligible in model **a**: the lowering effect is determined mostly by the conformations around ^{A}Se and ^{B}Se.

Some molecular orbitals of **a** (**BB**) and **b** (**BB**) seem well correspond to ψ_1, ψ_3, and ψ_4 of HSeOSeH 5c−6e (Figure 6). An approximate molecular orbital model of 5c−6e for the linear five H−Se- - -O- - -Se−H atoms, containing the characters of the models, is also depicted in Figure 6. It is well supported that the linear σ*(H−Se)- - -n_p(O)- - -σ*(Se−H) interactions in **a** (**BB**) and **b** (**BB**) is analyzed by the 5c−6e model.

The character of CT in 5c−6e of σ*(H−Se)- - -n_p(O)- - -σ*(Se−H) interactions in the models is further examined by the natural charges (*Qn*). Table 1 exhibits the *Qn* values for the $^{A}SeH_2$, $^{B}SeH_2$, O═CH_2, and/or OH_2 molecules in model **a** and model **b** calculated by the natural population analysis of the Gaussian program.[23] Table 1 tells that the direction of CT in model **a** is from H_2Se to O═CH_2 in type **A** and from O═CH_2 to H_2Se in type **B**. The magnitude of the latter is about two times larger than that of the former. CT is negligible in **b** (**AA**-cis) and from $H_2{}^{A}Se$ to H_2O in type **A** of **b** (**BA**), although not so large, and it is from H_2O to H_2Se in type **B** of **b** (**BA**) and **b** (**BB**). The magnitude of CT from H_2O to H_2-Se in **b** (**BB**) is about 1.7 times larger than that from CH_2═O to H_2Se in **a** (**BB**). The model calculations clarify the extended hypervalent 5c−6e character of the σ*(H−Se)- - -n_p(O)- - -σ*(Se−H) type in model **a** and model **b**.

After establishment of the extended hypervalent HSeOSeH 5c−6e character of the models, QC calculations are also performed on **1a**−**3a** in order to elucidate the CSeOSeC 5c−6e nature in **1** and **2**. The importance of the through π-conjugation to stabilize **1** (**BB**) is also shed light by the calculations, together with that of σ-type 5c−6e, on the structure.

Extended Hypervalent CSeOSeC 5c−6e in 1 and 2. Three conformers around the two Se atoms, type **A**−type **A**, type **A**−type **B**, and type **B**−type **B** pairings, are optimized to be stable for **1a**−**3a** when QC calculations are performed on **1a**−**3a** (Table 2 and Figure 7). Only the trans conformer of type **A**−type **A** is optimized for **1a**, only cis for **2a**, and both cis and trans for **3a**. While the observed structures are well reproduced to be most stable for **1a** and **2a** by the calculations, the observed **3a** (**AA**-cis) structure is predicted to be slightly less stable than **3a** (**AA**-trans) and **3a** (**AB**).

The conformers, **1a** (**AB**) and **1a** (**BB**), are evaluated to be more stable than **1a** (**AA**-trans) by 31.5 and 60.6 kJ mol^{-1}, respectively. Similarly, **2a** (**AB**) and **2a** (**BB**) are more stable than **2a** (**AA**-cis) by 24.4 and 36.5 kJ mol^{-1}, respectively. While the stabilization energies for the two processes from **1a** (**AA**-trans) to **1a** (**BB**) via **1a** (**AB**) are predicted to be almost equal (29−32 kJ mol^{-1}), that from **2a** (**AA**-cis) to **2a** (**AB**) and that from the latter to **2a** (**BB**) are very different, which are 24 and 12 kJ mol^{-1}, respectively. On the other hand, **3a** (**BB**) is evaluated to be most unstable among the four conformers, although the energy differences are very small

(26) Large deviation of a bromine atom from the anthracene plane is reported for 1,8,9-tri(bromo)anthracene.[8a] The 3c−6e nature of the σ-type interaction between atomic p-orbitals of the three bromine atoms in 1,8,9-tri(bromo)anthracene must play an important role in the deviation, in addition to the steric repulsion between the bromine atoms.

(27) Model **c** (H_2C═O- - -$^{A}SeH_aH_b$) and model **d** (H_2O- - -$^{A}SeH_aH_b$) are also constructed similarly to model **a** and model **b**, respectively. The type **B** structures are optimized to be more stable than the type **A** by 43.3 and 39.6 kJ mol^{-1} for model **c** and model **d**, respectively. The details will be reported elsewhere.

CHART 3 π-Conjugation between π(C═O) and n_{pz}(Se) through π-Framework in 1

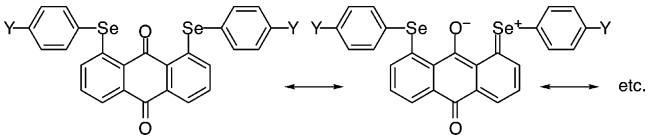

(<4 kJ mol^{-1}), which would be the reflection of the slightly disadvantageous steric effect in type **B** relative to type **A** in **3**. One may recognize that the contribution of 5c−6e to **1a** (**BB**) is larger than that to **2a** (**BB**) and the contribution is saturated in the process from **2a** (**AB**) to **2a** (**BB**), at first glance. However, we must be careful, since the contributions of 5c−6e are predicted to be very similar in the models, as discussed above.

Through π-interaction between n_{pz}(Se) and n_{pz}(O) via π-framework of anthraquinone in **1** must contribute to stabilize **1** (**BB**). Since the carbonyl groups in **1** act as good π-electron acceptors, the through π-interaction increases and decreases the electron densities at the O and Se atoms in **1**, respectively, relative to those without interactions. This will make advantageous conditions to strengthen the extended hypervalent 5c−6e interaction in **1**, since the 5c−6e interaction is of the σ*(C−Se)←n_p(O)→σ*(Se−C) type. Namely, the type **B**−type **B** pairing becomes more stable in **1**. Such through π-bond interaction contributes little in **2** (**BB**).

Molecular orbitals are shown to extend over the linear five C−Se- - -O- - -Se−C atoms in HOMO-2 of **1a** (**BB**) and HOMO-9 of **2a** (**BB**), whereas two n_p(Se) orbitals appear in the different molecular orbitals in HOMO-1 and HOMO-3 of **3a** (**AA**-cis) (Figure 8). The results demonstrate well the 5c−6e character of the linear σ*(C−Se)- - -n_p(O)- - -σ*(Se−C) interactions in **1a** (**BB**) and **2a** (**BB**).

The results of MO calculations on **1a**−**3a** are summarized as follows: (1) The type **B** structure is evaluated to be more stable than the type **A** for both **1a** and **2a**. (2) The type **B** structure is less stable than the type **A** in **3a**, although the energy difference is very small, which may come from the disadvantageous steric conditions in type **B** relative to those in type **A**. (3) The stability of type **B** relative to type **A** is greater in **1a** than that in **2a**, which must partly come from the π-conjugation between π(C═O) and n_{pz}(Se) through the π-framework of anthraquinone in **1a**: The π-conjugation is larger in **1a** (type **B**) of the rigid structure (Chart 3). (4) The magnitude of the π-conjugation would be almost equal in each process from **1a** (**AA**) to **1a** (**BB**) via **1a** (**AB**). On the other hand, (5) the more flexible structure around the MeO group in **2a** must be responsible for the different stabilization energies evaluated for the two processes in **2a**. The lack of the effective π-conjugation between n_p(O) and n_p(Se) through π-framework in **2a** (**BB**) must also play an important role in the energy profile of **2a**.

It is well demonstrated that the energy lowering effect of the extended hypervalent σ*(C−Se)- - -n_p(O)- - -σ*(Se−C) 5c−6e interaction is the main factor for the double type **B** structures of **1** and **2**. The contribution of the π-conjugation between π(C═O) and n_{pz}(Se) through π-framework of anthraquinone also plays an additional role in **1** (**BB**).

Experimental Section

1,8-Bis(phenylselanyl)anthraquinone (1a). To 3.00 g (9.61 mmol) of diphenyl diselenide in 40 mL of ethanol was added 1.10 g (29.10 mmol) of $NaBH_4$ under Ar atmosphere. To the solution was added 40 mL of benzene, and the solution was then distilled to ca. 25 mL. Then 80 mL of DMF was added, and the solution was distilled until the temperature of the solution was 110 °C. After the solution was cooled to 45 °C, 2.40 g (8.66 mmol) of 1,8-dichloroanthraquionone and 4.30 g (22.58 mmol) of CuI were added. The mixture was refluxed over 20 h and cooled to room temperature. After usual workup, the crude product was chromatographed on silica gel that was covered with a basic alumina layer on the top and recrystallized from ethanol−chloroform. **1a** gave 78% yield as dark red prisms: mp 199.0 °C (DSC); ^{1}H NMR δ 7.30 (d, J = 8.1 Hz, 2H), 7.41 (t, J = 7.8 Hz, 2H), 7.42−7.52 (m, 6H), 7.73−7.80 (m, 4H), 8.11 (d, J = 7.5 Hz, 2H); ^{13}C NMR ($CDCl_3$) δ 124.6, 129.2, 129.5, 129.8, 129.9, 132.5, 134.5, 134.6, 137.5 ($^2J_{Se-C}$ = 10.0 Hz,), 143.2, 182.9, 184.3. Anal. Calcd for $C_{26}H_{16}O_2Se_2$: C, 60.25; H, 3.11. Found: C, 60.32; H, 3.15.

1,8-Bis(*p*-chlorophenylselanyl)anthraquinone (1b). Following a method similar to that for **1a**, **1b** gave 65% yield as dark red prisms: mp 278.4 °C (DSC); ^{1}H NMR δ 7.26 (dd, J = 1.1, 8.1 Hz, 2H), 7.44 (t, J = 8.1 Hz, 2H), 7.44 (d, J = 8.3 Hz, 4H), 7.68 (d, J = 8.4 Hz, 4H), 8.12 (dd, J = 1.1, 7.5 Hz, 2H); ^{13}C NMR ($CDCl_3$) δ 124.9, 127.4, 129.8, 130.2, 132.8, 134.8, 134.3, 134.6, 136.1, 138.8 ($^2J_{Se-C}$ = 10.0 Hz,), 142.2, 182.6, 184.3. Anal. Calcd for $C_{26}H_{14}Cl_2O_2Se_2$: C, 53.18; H, 2.40. Found: C, 53.22; H, 2.48.

1,8-Bis(phenylselanyl)-9-methoxyanthracene (2a). To a solution of 2.00 g (5.45 mmol) of 1,8-dibromo-9-methoxyanthracene (**4**) in 30 mL of dry THF at −78 °C was added dropwise 7 mL of *n*-BuLi (1.6 M in hexane) via syringe, and the mixture was stirred at the same temperature for 2 h. Freshly prepared phenylselanyl bromide (2.84 g, 12.02 mmol) in 10 mL of dry THF was added to the orange suspension at −78 °C dropwise using canuula. The reaction mixture was maintained with stirring at −78 °C for 1.2 h, and then the temperature was raised to 65 °C slowly for 1 h. After usual workup, the crude product was chromatographed on silica gel with benzene/hexane = 1:1−4:1 eluent and recrystallization from ethanol−chloroform. **2a** gave 48% yield as yellow needles: mp 221.6 °C (DSC);, ^{1}H NMR ($CDCl_3$) δ 4.03 (s, 3H), 6.88 (dd, J = 0.6, 7.2 Hz, 2H), 7.10 (t, J = 7.8 Hz, 2H), 7.41−7.49 (m, 6H), 7.70 (d, J = 8.3 Hz, 2H), 7.77−7.84 (m, 4H), 8.17 (s, 1H); ^{13}C NMR ($CDCl_3$) δ 67.0, 123.7, 123.8, 125.3, 125.4, 125.8, 129.0, 129.3, 129.8, 131.6, 133.7, 137.9 ($^2J_{Se-C}$ = 10.6 Hz), 154.5. Anal. Calcd for $C_{27}H_{20}OSe_2$: C, 62.56; H, 3.89. Found: C, 62.61; H, 3.88.

1,8-Dibromo-9-methoxyanthracene (4).[28] To a solution of 77.74 g (1943.61 mmol) of NaOH and 3.82 g (11.84 mmol) of $(n\text{-Bu})_4$NBr in 250 mL of H_2O was added, dropwise and with vigorously stirring during 45 min, a solution of 13.29 g (37.74 mmol) of 1,8-dibromo-9-anthrone (**5**) and 19.92 g (157.92 mmol) of dimethyl sulfate in 215 mL of CH_2Cl_2. The resulting mixture was stirred at 25 °C for an additional 1.5 h. After usual workup, the crude product was recrystallized from chloroform−acetone to give 6.45 g of **4** as orange prisms (47% yield): mp 178.6 °C (DSC); ^{1}H NMR ($CDCl_3$) δ 3.86 (s, 3H), 7.24 (t, J = 7.7 Hz, 2H), 7.85 (d, J = 7.2 Hz, 2H), 7.91 (d, J = 8.3 Hz, 2H), 8.23 (s, 1H).

1,8-Dibromo-9-anthrone (5).[28] A 17.00 g (46.45 mmol) portion of 1,8-dibromoanthraquinone (**6**) was dissolved in 155 mL of concentrated sulfuric acid with vigorous stirring. Then 4.01 g (148.63 mmol) of Al powder was added, and the mixture was stirred for 42 h, while the temperature of the mixture was maintained at 30−40 °C. The resulting yellow suspension was poured onto 500 mL of ice−water and, after standing for 20 min, filtered. After usual workup, the crude product was

(28) House, H. O.; Hrabie, J. A.; VanDerveer, D. *J. Org. Chem.* **1986**, *51*, 921−929.

recrystallized from CH_2Cl_2−ethanol to give 13.54 g of **5** as tan needles (83% yield): ^{1}H NMR ($CDCl_3$) δ 4.17 (s, 2H), 7.29 (d, J = 7.7 Hz, 2H), 7.34 (t, J = 7.7 Hz, 2H), 7.64 (d, J = 7.7 Hz, 2H).

1,8-Dibromoanthraquinone (6).[29] To a suspension of 10.00 g (36.09 mmol) of 1,8-dichloroanthraquinone, 21.47 g (180.44 mmol) of KBr, and 0.43 g (2.53 mmol) of $CuCl_2 \cdot 2H_2O$ in 87 mL of nitrobenzene was added 11 mL of 85% H_3PO_4 with vigorously stirring, and then the solution was refluxed for 42 h. After one-third of the solution was steam distilled, cooled, and filtered, the residue was recrystallized from chloroform−ethanol to give 7.81 g of 6 as yellow prisms (59% yield): mp 235.9 °C (DSC); ^{1}H NMR ($CDCl_3$) δ 7.55 (t, J = 7.9 Hz, 2H), 8.03 (d, J = 7.9 Hz, 2H), 8.24 (dd, J = 1.3, 7.7 Hz, 2H).

1,8-Bis(phenylselanyl)anthracene (3a).[28] To 2.00 g (3.86 mmol) of **1a** in 60 mL of 1,4-dioxane were added 2.52 g (38.6 mmol) of zinc powder and 0.096 g (0.39 mmol) of $CuSO_4 \cdot 5H_2O$, and then 120 mL of 28% NH_3(aq) was added slowly. The solution was heated to reflux over 4 h. The solvent was removed in vacuo. The residue was dissolved in 80 mL of ethanol and 1 mL of 36% HCl(aq). The solution was heated to reflux during 1 h. The reaction mixture was concentrated in vacuo. The crude product was chromatographed on silica gel and recrystallized from ethanol. **3a** gave 86% yield as bright yellow prisms: mp 126.8 °C (DSC); ^{1}H NMR δ 7.12−7.18 (m, 6H), 7.32 (dd, J = 7.4, 8.4 Hz, 2H), 7.42−7.46 (m, 4H), 7.74 (dd, J = 1.1, 7.0 Hz, 2H), 7.94 (dd, J = 1.1, 8.5 Hz, 2H), 8.42 (s, 1H), 9.48 (s, 1H); ^{13}C NMR ($CDCl_3$) δ 125.8, 127.1, 127.4, 127.9, 128.9, 129.2, 131.0, 131.1, 132.2, 132.2, 132.8 ($^2J_{Se-C}$ = 11.8 Hz,), 133.3 ($^2J_{Se-C}$ = 8.7 Hz). Anal. Calcd for $C_{26}H_{18}Se_2$: C, 63.95; H, 3.72. Found: C, 63.89; H, 3.64.

1,8-Bis(*p*-chlorophenylselanyl)anthracene (3b).[28] Following a method similar to that for **3a**, **3b** gave 28% yield as bright yellow prisms: mp 167.1 °C (DSC); ^{1}H NMR δ 7.06 (d, J = 8.6 Hz, 4H), 7.27 (d, J = 8.6 Hz, 4H), 7.35 (t, J = 8.4 Hz, 2H), 7.80 (dd, J = 0.9, 6.8 Hz, 2H), 7.98 (d, J = 8.4 Hz, 2H), 8.40 (s, 1H), 9.41 (s, 1H), ^{13}C NMR ($CDCl_3$) δ 125.8, 127.6, 128.2, 129.3, 129.5, 129.6, 130.1, 132.2, 132.3, 133.2, 133.4 ($^2J_{Se-C}$ = 11.8 Hz,), 134.3 ($^2J_{Se-C}$ = 10.6 Hz,). Anal. Calcd for $C_{26}H_{16}Cl_2Se_2$: C, 56.04; H, 2.89. Found: C, 56.22; H, 2.98.

X-ray Structural Determination. The intensity data were collected on a Rigaku AFC5R four-circle diffractometer with graphite-monochromated Mo Kα radiation (λ = 0.710 69 Å) for **1a**, **2a**, and **3a**. The structures of **1a**, **2a**, and **3a** were solved by heavy-atom Patterson methods, PATTY[30] and SAPI91[31] and expanded using Fourier techniques, DIRDIF94.[32] All the non-hydrogen atoms were refined anisotropically. Hydrogen atoms were included but not refined. The final cycle of full-matrix least-squares refinement was based on a total of 2756 reflections for **1a**, on 2795 for **2a**, and on 3395 for **3a** with 271 observed reflections ($I > 1.50\sigma(I)$) for **1a**, 271 for **2a**, and 253 for **3a**, respectively. Variable parameters and converged with unweighted and weighted agreement factors of $R = (\Sigma||F_o| - |F_c||)/\Sigma|F_o|$ and $R_\omega = \{\Sigma\omega(|F_o| - |F_c|)^2/\Sigma\omega F_o^2\}^{1/2}$ were used. For least squares, the function minimized was $\Sigma\omega(|F_o|-|F_c|)^2$, where $\omega = (\sigma_c^2|F_o| + p^2|F_o|^2/4)^{-1}$. Crystallographic details are given in the Supporting Information.

MO Calculations. Ab initio molecular orbital calculations are performed on an Origin computer using Gaussian 94[17] and 98[18] programs with 6-311+G(3df,2pd) basis sets at the DFT (B3LYP) level for models. The 6-311+G(d) basis sets are employed for Se and O atoms, together with the 6-31G(d) basis sets for C and H atoms, in the MO calculations of **1a**, **2a**, and **3a**, using the B3LYP/Gen method.

Acknowledgment. This work was supported by a Grant-in-Aid for Scientific Research on Priority Areas (A) (Nos. 11120232, 11166246, and 12042259) from the Ministry of Education, Culture, Sports, Science, and Technology, Japan, by a Grant-in-Aid for Encouragement of Young scientists (No. 13740354) from the Japan Society for Promotion of Science, and by the Hayashi Memorial Foundation for Female Natural Scientists.

Supporting Information Available: X-ray crystallographic data of **1a**,**b**, **2a**, and **3a**,**b** (PDF and CIF). *Z*-Matrixes for models **a**−**d** optimized under given conditions with the B3LYP/6-311++G(3df,2pd) method. This material is available free of charge via the Internet at http://pubs.acs.org.

JO035393+

(29) Farbenindustrie, I. G. D. R. P. **1931**, 597259. *Frdl.* **21**, 1112.

(30) Beurskens, P. T.; Admiraal, G.; Beurskens, G.; Bosman, W. P.; Garcia-Granda, S.; Gould, R. O.; Smits, J. M. M.; Smykalla, C. The DIRDIF program system, Technical Report of the Crystallography Laboratory, University of Nijmegen, The Netherlands, 1992.

(31) Fan, H.-F. Structure Analysis Programs with Intelligent Control, Rigaku Corp., Tokyo, Japan, 1991.

(32) Beurskens, P. T.; Admiraal, G.; Beurskens, G.; Bosman, W. P.; de Gelder, R.; Israel, R.; Smits, J. M. M. The DIRDIF-94 program system, Technical Report of the Crystallography Laboratory, University of Nijmegen, The Netherlands, 1994.